

Size effect in fracture: roughening of crack surfaces and asymptotic analysis

Stéphane Morel,¹ Elisabeth Bouchaud,² and Gérard Valentin¹

¹ *Lab. de Rhéologie du Bois de Bordeaux, UMR 5103, Domaine de l'Hermitage, B.P.10, 33610 Cestas Gazinet, France*

² *C.E.A.- Saclay (DSM/DRECAM/SPCSI), 91130 Gif-Sur-Yvette Cedex, France*

Recently the scaling laws describing the roughness development of fracture surfaces was proposed to be related to the macroscopic elastic energy released during crack propagation¹³. On this basis, an energy-based asymptotic analysis allows to extend the link to the nominal strength of structures. We show that a Family-Vicsek scaling leads to the classical size effect of linear elastic fracture mechanics. On the contrary, in the case of an anomalous scaling, there is a smooth transition from the case of no size effect, for small structure sizes, to a power law size effect which appears weaker than the linear elastic fracture mechanics one, in the case of large sizes. This prediction is confirmed by fracture experiments on wood.

I. INTRODUCTION

In solid mechanics, an essential scaling problem is the effect of the structure size on its nominal strength. This effect is particularly important in the case of *quasibrittle* materials which are characterized by the existence of a large fracture process zone containing many damage microcracks. Materials as different as concretes, mortar and rocks, some composites, toughened ceramics and wood belong to this category. Bažant^{1,2} has shown that in this case, contrary to what happens for Weibull's statistics³, the size effect is linked to the very existence of the development of such a large microcracked zone, which implies stress redistributions and stored energy release.

On the other hand, in quasibrittle materials, damage has a strong influence on the local deviations of the main crack through its elastic interactions with the microcracks⁴⁻⁶. Consequently, the roughness of the fracture surfaces can be considered as an inheritance of the damage process and it is naturally tempting to correlate their morphology (and especially their fractal properties) to macroscopic mechanical properties such as fracture energy or fracture toughness⁷⁻¹³.

In this paper, on the basis of a link recently established¹³ between the roughening of crack surfaces and the macroscopic energy released during crack propagation (this work is summarized in Section II), we propose an energy-based asymptotic analysis in Section III which allows to extend this link to the nominal strength of large (Sec. III A) and small (Sec. III B) structures. An approximate size effect valid everywhere is proposed in Sec. III C. This prediction is shown to be in agreement with experimental results obtained on wood Sec. IV. Finally, we discuss material-dependent properties in Sec. V.

II. SCALING LAWS OF CRACK SURFACES AND ENERGY RELEASE RATE

The statistical characterization of the fractal morphology of fracture surfaces is nowadays a very active field of research. It is now well established that these surfaces, for very different types of materials (from ductile aluminium alloys^{14,15} to brittle materials like rock^{17,16,18} or wood^{19,20}), exhibit self-affine scaling properties in a large range of lengthscales (see²¹ for a more detailed account of experiments). Moreover, in addition to this self-affine character, recent studies focussed on the complete description (3D) of the morphology of crack surfaces^{18,20} have shown that the scaling laws governing the crack developments in longitudinal and transverse directions are different and material dependent²⁰.

Let us consider the development of a fracture surface from a straight notch of length L with zero roughness. The mean plane of the crack surface is defined as (x, y) where the x axis is perpendicular to the direction of crack propagation and the y axis is parallel to this direction. For two quasibrittle materials (granite¹⁸ and wood²⁰), it has been found that the fluctuations Δh of the height on the fracture surfaces, estimated over a window of size l along the x axis and at a distance y from the initial notch exhibited *anomalous* scaling properties which are quite similar to those obtained in some models of nonequilibrium kinetic roughening^{22,23}:

$$\Delta h(l, y) \simeq A \begin{cases} l^{\zeta_{loc}} \xi(y)^{\zeta - \zeta_{loc}} & \text{if } l \ll \xi(y) \\ \xi(y)^{\zeta} & \text{if } l \gg \xi(y) \end{cases} \quad (1)$$

where $\xi(y) = By^{1/z}$ depends on the distance y to the initial notch and characterizes a crossover length along the x axis. For length scales smaller than $\xi(y)$, the surface is self-affine, and characterized by the local roughness exponent

ζ_{loc} . This self-affine character is observed in most experiments and a local roughness exponent $\zeta_{loc} \simeq 0.8$ is reported in all cases. Hence, it has been suggested that this local roughness exponent might be a universal index, *i.e.* independent of the fracture mode and of the material¹⁵.

According to Eq. (1), the magnitude of the roughness increases as a function of the distance y until the self-affine correlation length $\xi(y)$ reaches the system size L . This happens at a certain distance $y_{sat} = (L/B)^z$ from the notch: $\xi(y \gg y_{sat}) = L$. Thus, the first growth regime of the roughness (*i.e.* for $y \ll y_{sat}$) is followed by a stationary regime (for $y \gg y_{sat}$) where the magnitude of the roughness remains constant and where the global roughness (*i.e.* measured over the system size L) is driven by the global roughness exponent ζ : $\Delta h(L, y \gg y_{sat}) \sim L^\zeta$. The main consequence of an anomalous scaling [Eq. (1)] is that, in this stationary regime, the magnitude of the local roughness (*i.e.* measured on windows $l \ll L$) is not only a function of the window size l but also of the system size L : $\Delta h(l, y \gg y_{sat}) \sim l^{\zeta_{loc}} L^{\zeta - \zeta_{loc}}$.

Experimental results obtained on quasibrittle materials have shown the following values for the global roughness exponent: $\zeta = 1.2$ for granite¹⁸ and 1.35 and 1.60 for wood (pine and spruce respectively)²⁰. Note that the exponent z (called the “dynamic exponent”) and the prefactors A and B seem also to be material-dependent²⁰.

The Family-Vicsek scaling law²⁴, where the height fluctuations Δh scale as:

$$\Delta h(l, y) \simeq A \begin{cases} l^{\zeta_{loc}} & \text{if } l \ll \xi(y) \\ \xi(y)^{\zeta_{loc}} & \text{if } l \gg \xi(y) \end{cases} \quad (2)$$

can be seen as a particular case of the anomalous scaling [Eq. (1)] where $\zeta = \zeta_{loc}$. In this case [Eq. (2)], the magnitudes of the local and global roughnesses at saturation, respectively $\Delta h(l, y \gg y_{sat}) \sim l^{\zeta_{loc}}$ and $\Delta h(L, y \gg y_{sat}) \sim L^{\zeta_{loc}}$, are driven by the same roughness exponent (the local roughness exponent ζ_{loc}). Furthermore, the local roughness is independent of the system size. This is drastically different from what happens in the case of an anomalous scaling. It is worth noticing that both the Family-Vicsek and the anomalous scaling laws were used to describe the roughness development of the same granite fracture surface^{17,18}, and that more accurate results were obtained assuming anomalous scaling¹⁸.

The anomalous and Family-Vicsek scalings were recently shown to be linked to drastically different mechanical behaviors in terms of elastic energy release¹³. Within the framework of an equivalent linear elastic problem, a fracture criterion, linking the elastic energy release rate G at the macroscale and the fractal nature of the crack at the microscale, was proposed: $G = 2\gamma\psi(y)/L$. In this fracture criterion, γ is the so-called specific surface energy and the ratio $\psi(y)/L$ can be considered as a “roughness factor”. As a matter of fact, it is precisely the ratio of the length of a *virtual* crack front over its projected length L (the system size, *i.e.* the specimen width). This virtual front, parallel to the initial notch, is assumed to be rough only out of the average fracture plane (x, y) , and this roughness can be defined from the functions $\Delta h(l, y)$ at a fixed position y from the initial notch.

According to an anomalous scaling [Eq. (1)], the estimate of the real length ψ of the virtual front (which corresponds to the length of a self-affine curve¹³) leads to the following expressions of the energy release rate:

$$G_R(\Delta a) \simeq 2\gamma \begin{cases} \sqrt{1 + \left(\frac{AB^{\zeta - \zeta_{loc}}}{l_o^{1 - \zeta_{loc}}}\right)^2 \Delta a^{2(\zeta - \zeta_{loc})/z}} & \text{if } \Delta a \ll \Delta a_{sat} \\ \sqrt{1 + \left(\frac{A}{l_o^{1 - \zeta_{loc}}}\right)^2 L^{2(\zeta - \zeta_{loc})}} & \text{if } \Delta a \gg \Delta a_{sat} \end{cases} \quad (3)$$

where the crack length increments Δa and Δa_{sat} defined from the initial notch correspond respectively to the crack positions y and y_{sat} defined in Eq. (1). In the zone where the roughness grows, *i.e.* for $\Delta a \ll \Delta a_{sat}$, the fracture equilibrium leads to an energy release rate function of the crack length increment Δa [Eq. (3)]. The subscript R in G_R emphasizes the fact that the resistance to fracture growth is similar to the behavior described by a resistance curve (usually called R -curve⁶). Note that the square root terms in Eq. (3) are dimensionless and correspond to the roughness factor $\psi(y)/L$. The term l_o is the lower cutoff of the fractal range of the virtual front (*i.e.* the characteristic size of the smaller microstructural element relevant for the fracture process). When the crack increment is large, *i.e.* for $\Delta a \gg \Delta a_{sat}$ [Eq. (3)] which corresponds to the saturation state of the roughness, the resistance to fracture growth becomes independent of the crack length increment because the self-affine correlation length has reached the system size: $\xi(\Delta a \gg \Delta a_{sat}) \simeq L$. Introducing the crossover length $L_C = (l_o^{1 - \zeta_{loc}}/A)^{1/(\zeta - \zeta_{loc})}$, the resistance to crack growth for large crack length increments becomes:

$$G_R(\Delta a \gg \Delta a_{sat}) \simeq G_{RC} \simeq 2\gamma \sqrt{1 + \left(\frac{L}{L_C}\right)^{2(\zeta - \zeta_{loc})}} \quad (4)$$

where the subscript C in G_{RC} emphasizes that the resistance to crack growth has reached an asymptotic or *critical* value. The main consequence of the link between fracture mechanics and anomalous roughening of fracture surfaces¹³

is the size effect on the critical resistance to crack growth [Eq. (4)]. This size effect is the result of the dependence of the maximum magnitude of the roughness at saturation on the structure size L . As shown in Fig. 1, the size effect affecting the critical resistance G_{RC} exhibits two asymptotic behaviors separated by the crossover length L_C . For small structure sizes (*i.e.* $L \ll L_C$) where the roughness of the fracture surface is weak, there is no size effect, and $G_{RC} \simeq 2\gamma$. For large structure sizes (*i.e.* $L \gg L_C$), corresponding to an important fracture roughness, the critical resistance evolves as a power law : $G_{RC} \sim L^{\zeta - \zeta_{loc}}$.

In the case of the Family-Vicsek scaling [Eq. (2)], on the contrary, the link between roughening of fracture surfaces and material fracture properties¹³ reduces to a resistance to crack growth independent of the crack increment Δa and of the specimen size L :

$$G_C(\Delta a) \simeq 2\gamma \sqrt{1 + \left(\frac{A}{l_o^{1-\zeta_{loc}}}\right)^2} \quad (5)$$

Thus, an anomalous scaling accounts for an R -curve behavior and a size effect on the critical resistance to crack growth while a Family-Vicsek scaling reflects a purely elastic brittle fracture behavior.

III. SIZE EFFECT ON THE NOMINAL STRENGTH

We now extend the connection just summarized¹³ to the nominal strength of structures.

Within the framework of Bažant's theory²⁵, the size effect (for two-dimensional problem) can be described from geometrically similar structures of different sizes (with geometrically similar initial cracks or notches) by introducing a nominal stress:

$$\sigma_N = \frac{P}{dL} \quad (6)$$

where P is the external load applied to the structure (considered to be a load independent of the displacement), L is the characteristic size of the structure, and d is any length of the structure (for instance, as shown in Fig. 2 in the case of TDCB specimens, d corresponds to the ligament length). When $P = P_u$ which corresponds to the ultimate or maximum load, σ_N is called the *nominal strength* of the structure.

On the other hand, at the maximum load P_u , the elastic energy release rate G (obtained at a constant load P_u or σ_N) must be equal, according to the linear elastic fracture mechanics (LEFM), to the critical resistance to crack growth G_{RC} :

$$G = \frac{1}{L} \left[\frac{\partial W^*}{\partial a} \right]_{\sigma_N} = G_{RC} \quad (7)$$

where the complementary energy W^* characterizes the energy stored in the structure. This energy W^* can be written in the following form: $W^* = \sigma_N^2 L d^2 f(\alpha)/E$ where f is a dimensionless function characterizing the geometry of the structure and $\alpha = a/d$ is the relative crack length. Thus, when the maximum load is reached, the nominal strength of the structure can also be written as:

$$\sigma_N = \sqrt{\frac{E G_{RC}}{d g(\alpha)}} \quad (8)$$

where $g(\alpha) = \partial f(\alpha)/\partial \alpha$ corresponds to the dimensionless energy release rate function.

Usually, the main problem with Eq. (8) is to determine the relative crack length $\alpha = a/d$ for which the maximum load P_u is reached. Let us consider exclusively a structure of “positive geometry”, *i.e.* $\partial g(\alpha)/\partial \alpha > 0$ under load control.

If the material exhibits a purely elastic brittle behavior such as the one obtained for a Family-Vicsek scaling [Eq. (5)], the relative crack length increment α at the maximum load corresponds to $\alpha_o = a_o/d$ (a_o being the length of the notch or initial crack). Thus, in the case of a Family-Vicsek scaling, replacing the resistance to crack growth G_C by its expression in [Eq. 5] and α by α_o in Eq. (8), we obtain the following size effect relation:

$$\sigma_N = \sqrt{\frac{2\gamma E}{m g(\alpha_o)} \left[1 + \left(\frac{A}{l_o^{1-\zeta_{loc}}}\right)^2 \right]^{1/2}} L^{-1/2} \quad (9)$$

where m is a proportionality coefficient between d and L ($d = mL$). In Eq.(9), the term under the square root is a constant, which means that the nominal strength of structures evolves as $\sigma_N \sim L^{-1/2}$. This is in agreement with the expected LEFM size effect, *i.e.* the size effect of a purely elastic brittle fracture behavior.

In the case of an anomalous scaling, the problem appears more complicated. Indeed, under the conditions evoked in the previous case (*i.e.*, structures of positive geometry and under load control), if the material exhibits an R -curve behavior [Eq. (3)], the crack length increment Δa_{sat} (limit of the R -curve) is actually the limit of stability. Thus, the relative crack length at the maximum load can be defined as $\alpha = \alpha_o + \theta$ where $\theta = \Delta a_{sat}/d$. Hence, in the case of an anomalous scaling, which reflects the fracture behavior of quasibrittle materials, the knowledge of the evolution of the crack length increment Δa_{sat} as a function of the structure size is the key of the size effect problem. However, the dependence between Δa_{sat} and the specimen size does not appear clearly from the roughness analysis^{18,20}.

In order to resolve this problem - which is the central point of this paper -, a possible way suggested by Bažant²⁵ consists in considering that the failure of a quasibrittle material is not only characterized by the specific surface energy 2γ (related to the actual crack surface), but also by a critical damage energy release rate G_d per unit volume of *damaged* material (*i.e.* per unit volume of fracture process zone). Thus, one can assume that failure at the maximum load is obtained for the energy balance:

$$G_d V_{FPZ} = 2\gamma A_r(\Delta a_{sat}) \quad (10)$$

where the volume of the fracture process zone can be estimated as $V_{FPZ} = L \Delta a_{sat}^2/n$ with $L \Delta a_{sat}$ the projected crack surface and $\Delta a_{sat}/n$ the *height* of the process zone (where n is assumed constant, *i.e.* independent of the size L). The surface $A_r(\Delta a_{sat})$ corresponds to the real fracture surface produced during the crack advance Δa_{sat} . Note that the fracture criterion [Eq. (10)] actually corresponds to an equivalent linear elastic problem^{25,26} where the effective size of the fracture process zone at the maximum load is assumed equal to the crack length increment for which the resistance to crack growth does not follow the R -curve [Eq. (3)] but remains constant and equal to the critical resistance: $G_R(\Delta a_{sat}) = G_{RC}$ [Eq. (4)].

In the following, on the basis of the fracture criterion defined in Eq. (10), the asymptotic values of Δa_{sat} are estimated for large and small structures in order to obtain the nominal strength respectively for large and small-size asymptotic expansions.

A. Large-size asymptotic expansion of the size effect

As previously mentioned, the square root terms in Eq. (3) and Eq. (4) correspond to the ratio of the virtual crack front length $\psi(\Delta a)$ over its projected length L . Moreover, from Eq. (4), relative to the roughness saturation regime, one can obtain the maximum length of the virtual crack front since $\psi(\Delta a \gg \Delta a_{sat}) \simeq \psi_{max} \simeq L\sqrt{1 + (L/L_C)^{2(\zeta - \zeta_{loc})}}$ ¹³. Thus, for large structure sizes, *i.e.* $L \gg L_C$, the asymptotic value of the real crack surface A_r produced for a crack advance Δa_{sat} can be estimated from ψ_{max} as: $A_r \simeq \beta L \Delta a_{sat} (L/L_C)^{\zeta - \zeta_{loc}}$ where β is a constant (function of the scaling exponents). Substituting A_r in Eq. (10) yields the expression of the crack length increment:

$$\Delta a_{sat} = c^* \beta \left(\frac{L}{L_C} \right)^{\zeta - \zeta_{loc}} \quad (11)$$

where $c^* = n2\gamma/G_d$ is a material-dependent length scale. Thus, for large structure sizes, the relative size of the fracture process zone (*i.e.* $\theta = \Delta a_{sat}/d$) is expected to evolve as a power law $\theta \sim L^{\zeta - \zeta_{loc} - 1}$. Moreover, from the values of the scaling exponents obtained in the roughness analysis of quasibrittle materials^{18,20}, it appears that the relative size of the process zone becomes negligible when the system size increases: $\lim \theta = 0$ for $L \rightarrow +\infty$. In other terms, in large structures, the process zone is expected to lie within only an infinitesimal volume fraction of the body and so $\lim \alpha = \alpha_o$ for $L \rightarrow +\infty$. Note that this result is in agreement with Bažant's assumption²⁵. Hence, the dimensionless energy release rate function $g(\alpha)$ being generally a smooth function, we may expand it into a Taylor series around $\alpha = \alpha_o$ and Eq.(8) thus yields :

$$\sigma_N = \sqrt{\frac{E G_{RC}}{d}} \left[g(\alpha_o) + g_1(\alpha_o) \theta + g_2(\alpha_o) \frac{\theta^2}{2!} + g_3(\alpha_o) \frac{\theta^3}{3!} + \dots \right]^{-1/2} \quad (12)$$

$$= \sigma_M \sqrt{\frac{\left(1 + \left(\frac{L}{L_C} \right)^{2(\zeta - \zeta_{loc})} \right)^{1/2}}{\frac{L}{L_1} + \left(\frac{L}{L_C} \right)^{\zeta - \zeta_{loc}} + b_2 \frac{L_1}{L} \left(\frac{L}{L_C} \right)^{2(\zeta - \zeta_{loc})} + b_3 \left(\frac{L_1}{L} \right)^2 \left(\frac{L}{L_C} \right)^{3(\zeta - \zeta_{loc})} + \dots}} \quad (13)$$

where $g_1(\alpha_o) = \partial g(\alpha_o)/\partial \alpha$, $g_2(\alpha_o) = \partial^2 g(\alpha_o)/\partial \alpha^2$, ..., and $b_2 = g(\alpha_o)g_2(\alpha_o)/(2g_1(\alpha_o)^2)$, $b_3 = g(\alpha_o)^2 g_3(\alpha_o)/(6g_1(\alpha_o)^3)$, ..., and,

$$\sigma_M = \sqrt{\frac{2\gamma E}{mg(\alpha_o)L_1}}, \quad L_1 = c^* \frac{\beta}{m} \frac{g_1(\alpha_o)}{g(\alpha_o)} \quad (14)$$

are all constants. Equation (13) provides a large-size asymptotic series expansion of the size effect because the terms containing non zero powers of L in denominator vanish for $L \rightarrow \infty$. Note that Eq. (13) is expected to diverge for structure sizes $L \rightarrow 0$ as shown in Fig. 3. A first-order asymptotic approximation at large sizes can be obtained by truncating the series after the linear term:

$$\sigma_N = \sigma_M \sqrt{\frac{\left(1 + \left(\frac{L}{L_C}\right)^{2(\zeta - \zeta_{loc})}\right)^{1/2}}{\frac{L}{L_1} + \left(\frac{L}{L_C}\right)^{\zeta - \zeta_{loc}}} \quad (15)$$

The main consequence of the anomalous roughening in the case of large structure sizes is that the nominal strength is expected to decrease as $\sigma_N \sim L^{-1/2 + (\zeta - \zeta_{loc})/2}$ (as shown in Fig. 3). This result disagrees with the size effect proposed by Bažant²⁵ where the nominal strength of large structures decreases as $\sigma_N \sim L^{-1/2}$ which is the theoretical size effect of LEFM. The difference originates in the fact that, for an anomalous roughening, the critical resistance to crack growth G_{RC} [Eq. (4)] is expected to evolve as a power law $G_{RC} \sim L^{\zeta - \zeta_{loc}}$ for large structure sizes while in LEFM, the critical resistance G_{RC} is assumed to be constant (*i.e.* independent of the specimen size). Hence, the size effect on the nominal strength obtained for an anomalous roughening is weaker than the size effect in LEFM.

B. Small-size asymptotic expansion of the size effect

In Bažant's theory²⁵, no size effect is expected for small structure sizes ($L \rightarrow 0$); this is the domain of the strength theory. A possible justification is that, in small structures, the fracture process zone fills the whole volume of the structure and hence, there is no stress concentration and, as a consequence, failure occurs with no crack propagation.

Such an argument can be also obtained from the link between anomalous roughening of crack surfaces and material fracture properties. Indeed, in small structure sizes (*i.e.* $L \ll L_C$), the roughness being negligible, the virtual crack front length tends to its projected length L . This implies that, for small structures, the actual crack surfaces produced during a crack advance Δa_{sat} are not so different from the projected one: $A_r \simeq L\Delta a_{sat}$. Hence, substituting $A_r \simeq L\Delta a_{sat}$ into the fracture criterion [Eq. (10)] yields the crack length increment: $\Delta a_{sat} = n2\gamma/G_d = c^*$ for $L \ll L_C$. In other terms, the effective size of the process zone tends to the material length for small structure sizes. Thus, when the material length $c^* = d - a_o$ (Fig. 2), the fracture process zone occupies the entire ligament of the structure.

On the basis of Bažant's theory²⁵ and in order to obtain a small-size asymptotic expansion of the size effect, let us now introduce a new variable and a new function:

$$\eta = \frac{1}{\theta} = \frac{d}{\Delta a_{sat}}, \quad \varphi(\alpha_o, \eta) = \frac{g(\alpha_o + \theta)}{\theta} = \eta g(\alpha_o + 1/\eta) \quad (16)$$

The function $\varphi(\alpha_o, \eta)$ corresponds to the dimensionless energy release rate function of the inverse relative size of the process zone. Substituting Eq. (16) into Eq. (8) and expanding $\varphi(\alpha_o, \eta)$ into Taylor series around the point $(\alpha_o, 0)$ since $\lim \eta = 0$ when d or $L \rightarrow 0$, yields the nominal strength:

$$\sigma_N = \sqrt{\frac{E G_{RC}}{c^*}} \left[\varphi(\alpha_o, 0) + \varphi_1(\alpha_o, 0) \eta + \varphi_2(\alpha_o, 0) \frac{\eta^2}{2!} + \varphi_3(\alpha_o, 0) \frac{\eta^3}{3!} + \dots \right]^{-1/2} \quad (17)$$

$$= \sigma_{M'} \sqrt{\frac{\left(1 + \left(\frac{L}{L_C}\right)^{2(\zeta - \zeta_{loc})}\right)^{1/2}}{1 + \frac{L}{L_2} + c_2 \left(\frac{L}{L_2}\right)^2 + c_3 \left(\frac{L}{L_2}\right)^3 + \dots}} \quad (18)$$

where $\varphi_1(\alpha_o, 0) = \partial \varphi(\alpha_o, 0)/\partial \eta$, $\varphi_2(\alpha_o, 0) = \partial^2 \varphi(\alpha_o, 0)/\partial \eta^2$, ..., and $c_2 = \varphi_2(\alpha_o, 0)\varphi(\alpha_o, 0)^2/(2\varphi_1(\alpha_o, 0)^2)$, $c_3 = \varphi_3(\alpha_o, 0)\varphi(\alpha_o, 0)^3/(6\varphi_1(\alpha_o, 0)^3)$, ..., and,

$$\sigma_{M'} = \sqrt{\frac{2\gamma E}{\varphi(\alpha_o, 0)c^*}}, \quad L_2 = c^* \frac{\varphi(\alpha_o, 0)}{m \varphi_1(\alpha_o, 0)} \quad (19)$$

are all constants. Equation (18) provides a small-size asymptotic series expansion of the size effect and is plotted in Fig. 3. When $L \rightarrow 0$, the nominal strength tends to a constant (*i.e.* $\sigma_{M'}$ as expected in the case of a strength theory²⁵) but diverges from the asymptotic behavior of the size effect obtained in the case of large structure sizes [Eq. (13)].

C. Approximate size effect

Now, the main problem consists in interpolating between the large-size [Eq. (13)] and the small-size [Eq. (18)] asymptotic series expansion in order to obtain an approximate size effect valid everywhere. The theory of intermediate asymptotics²⁷ is not easily applicable in our case. Nevertheless, it is interesting to observe in Fig. 3 that a satisfactory approximate size effect can be obtained by truncating the small-size asymptotic series expansion [Eq. (18)] after the linear term:

$$\sigma_N = \sigma_{max} \sqrt{\frac{\left(1 + \left(\frac{L}{L_C}\right)^{2(\zeta - \zeta_{loc})}\right)^{1/2}}{1 + \frac{L}{L_o}}} \quad (20)$$

where the constants σ_{max} and L_o will be discussed in what follows. Indeed, Eq. (20) allows to obtain the transition between a horizontal asymptote characterizing the strength theory for which there is no size effect, and a decreasing asymptote, corresponding to a power law of exponent: $-1/2 + (\zeta - \zeta_{loc})/2$ for large structure sizes. A possible justification is that, in the large-size first-order expansion [Eq. (15)], the second term in numerator has no influence on the power law $\sigma_N \sim L^{-1/2 + (\zeta - \zeta_{loc})/2}$ for large sizes but induces a divergence at small sizes.

One limitation of the approximate size effect is that in Eq. (20), the values of σ_M and $\sigma_{M'}$, and the values of L_1 and L_2 , are assumed to be equal and respectively characterized by σ_{max} and L_o . Indeed, the estimate of these values would be surely different from large size data or from small size data. Thus, the approximate size effect only gives the shape of the size effect relation on the nominal strength but does not allow for a determination of the parameter values σ_{max} and L_o . Only the crossover length L_C and the scaling exponents ζ_{loc} and ζ are univocally determined from the roughness analysis. However, it seems reasonable to assume that the difference between σ_M and $\sigma_{M'}$ will be masked by the scatter of the experimental data. On the other hand, it seems difficult to compare the crossover lengths L_1 and L_2 (characterized by L_o in Eq. (20)) to the crossover length L_C using their analytical expressions, because the former is deduced from a mechanical approach and the latter from a roughness analysis. Nevertheless, from a physical point of view, both have the same meaning. For small structure sizes, *i.e.* $L \ll L_C$ or L_o , the energy released by the structure is negligible, while for large sizes, *i.e.* $L \gg L_C$ or L_o , the energy released is dominant. Hence, it seems reasonable to assume that both crossover lengths are of the same order of magnitude (it is the case in Fig. 3 where it is assumed that $L_o = L_C$).

IV. EXPERIMENT

In the following the experimental setup of mode I fracture tests on a quasibrittle material, wood, is described. Two wood species have been tested: Maritime pine (*Pinus pinaster Ait*) and Norway spruce (*Picea Abies L.*). The average oven dry specific densities were respectively 0.55 and 0.40 and the moisture content of all specimens was measured between 11 and 13 %. Tests were made on modified tapered double cantilever beam specimens (TDCB) oriented along the longitudinal-tangential directions of wood (Fig. 2). Six sets of geometrically similar specimens characterized by their width $L = 7.5, 11.3, 15.0, 22.5, 30.0$ and 60.0 mm have been used. A straight notch is machined with a band saw (thickness 2 mm) and prolonged a few millimeters with a razor blade (thickness 0.2 mm). Fracture is obtained through uniaxial tension at a constant opening rate. The fracture surfaces are generated along the average longitudinal-radial plane of wood. Load-deflection values were continuously recorded during the tests.

The roughness analysis²⁰, performed from these fracture tests, has shown an anomalous roughening [Eq. (1)] of the crack surfaces driven by the global and local roughness exponents, $\zeta = 1.35 \pm 0.10$ and $\zeta_{loc} = 0.88 \pm 0.07$ in the case of pine, and, $\zeta = 1.60 \pm 0.10$ and $\zeta_{loc} = 0.87 \pm 0.07$ in the case of spruce. Hence, the experimental *R*-curve behaviors and the size effects on critical energy release rates and nominal strengths should be described respectively by Eq. (3), Eq. (4) and Eq. (20).

From an equivalent linear elastic approach (which is the frame of the model described in Sec. II and Sec.III) where the crack lengths can be estimated from the unloading compliance of the specimens, the elastic energy release rate G_R are computed from the load-deflection curves for any crack length increment Δa . Two examples of the energy release rate evolution G_R as a function of the crack length extension Δa obtained for both wood species and for a specimen size $L = 11.3 \text{ mm}$ are given in Fig. 4. An R -curve behavior is observed for both wood species, *i.e.* a pronounced evolution of the resistance to crack growth as a function of the equivalent crack length increment⁶. After a characteristic propagation distance ($\Delta a_{sat} \simeq 23 \text{ mm}$ for pine (a) and 40 mm for spruce (b)) which corresponds approximately to the ultimate load P_u , the energy release rate becomes independent of the crack length increment Δa . The post R -curve behavior arises at constant resistance to crack growth and corresponds to critical resistance G_{RC} . In Figure 4 the R -curves and post R -curve behaviors are fitted with the Eq. (3). These fits are obtained in keeping three free parameters: the specific surface energy γ , the ratio $A/l_o^{1-\zeta_{loc}}$ and the scaling exponent $(\zeta - \zeta_{loc})/z$. The expected R -curve behavior [Eq. (3)] provides a good description of the increase of the experimental resistances to crack growth. For both wood species, the fitted exponents $(\zeta - \zeta_{loc})/z$ are close to those measured from the roughness analysis²⁰ which are given in brackets in Fig. 4. Note that the R -curve is more pronounced in pine than in spruce (*i.e.* the critical energy release rate G_{RC} is greater for a smaller crack length increment Δa_{sat} than in spruce). This trend has also been observed for the other specimen sizes L .

On the other hand, for both wood species, it has been shown that the sizes L of tested specimens were greater than the crossover lengths L_C ¹³ [defined in Eq.(4) and Eq. (20) relative to the size effect]. Thus, according to Eq. (4) and for $L \gg L_C$, the size effect on the critical energy release rates of both wood species is expected to evolve as a power law: $G_{RC} \sim L^{\zeta - \zeta_{loc}}$. The critical energy release rates obtained for both wood species are plotted in Fig. 5 versus the characteristic specimen sizes L . Experimental size effects are fitted by a power law $G_{RC}(L) \sim L^\beta$ whose the exponents $\beta = 0.42$ for pine (a) and $\beta = 0.64$ for spruce (b) are in fair agreement with the expected exponents $\zeta - \zeta_{loc} = 0.47 \pm 0.17$ for pine (a) and 0.73 ± 0.17 for spruce (b). Note that the size effect on critical energies of spruce is stronger than the one obtained for pine.

In the same way, in Fig. 6, the nominal strengths σ_N obtained for both wood species are plotted versus the characteristic specimen sizes L . According to Eq. (20) and, as previously mentioned for $L \gg L_C$, the size effect on nominal strengths is expected to evolve as: $\sigma_N \sim L^{-1/2 + (\zeta - \zeta_{loc})/2}$. Note that latter asymptotic behaviour is obtained with the assumption $L_o = L_C$ in Eq. (20) as previously discussed in Sec III C. As shown in Fig. 6, simple power law fits of the experimental nominal strengths give exponent which are in good agreement with those expected, *i.e.* $-\frac{1}{2} + \frac{\zeta - \zeta_{loc}}{2} = -0.27 \pm 0.09$ for pine (a) and -0.14 ± 0.09 for spruce (b). By comparison of the size effects on the critical energy release rates and on the nominal strengths it is appeared that, as expected intuitively, the more the size effect on critical energies is important the more the size effect on nominal strengths is weak.

V. CONCLUSION

From an energy-based analysis, a link between the scaling laws describing the fracture surfaces and the size effect on the nominal strength of the structures is proposed. On the basis of a Family-Vicsek scaling, which has been shown to reflect a purely elastic brittle fracture behavior¹³, the size effect obtained is in agreement with the classical size effect of linear elastic fracture mechanics: $\sigma_N \sim L^{-1/2}$ [Eq. (9)]. In the case of an anomalous scaling, reflecting the fracture behavior of quasibrittle materials¹³, an asymptotic analysis allows to estimate the size effect relation on the nominal strength, and especially, the crack length increment for which the maximum load is reached. From large-size and small-size asymptotic series expansion of the size effect, an approximate size effect [Eq. (20)] of general validity is proposed. This relation represents a smooth transition from the case of no size effect, for small structure sizes, to a power law size effect which appears weaker than the size effect of LEFM. Thus, in the case of quasibrittle materials, the approximate size effect relation [Eq. (20)] is different from the *classical* size effect law proposed by Bažant²⁵ and especially for large structure sizes where an asymptotic behavior $\sigma_N \sim L^{-1/2 + (\zeta - \zeta_{loc})/2}$ is predicted instead of the size effect of LEFM suggested by Bažant's theory. The difference can be explained by the fact that, for an anomalous scaling of fracture surfaces, the critical resistance to crack growth at the maximum load evolves as a power law $G_{RC} \sim L^{\zeta - \zeta_{loc}}$ for large structure sizes while this resistance is assumed to be constant in LEFM. Experiments performed on geometrically similar wood specimens of various sizes, for which anomalous roughening of crack surfaces has been observed previously²⁰, show that the size effects on the critical resistances and on the nominal strengths are in fair agreement with the predicted asymptotic behaviors $G_{RC} \sim L^{\zeta - \zeta_{loc}}$ and $\sigma_N \sim L^{-1/2 + (\zeta - \zeta_{loc})/2}$. On the other hand, if one considers a *weakly* anomalous roughening of the fracture surfaces (*i.e.* $\zeta \rightarrow \zeta_{loc}$), R -curve [Eq. (3)] and size effect on the critical resistance [Eq. (4)] vanish progressively and as a consequence, the size effect characteristic of a quasibrittle material [Eq. (20)] tends to the classical size effect of a purely elastic brittle material [Eq. (9)]. Experiments on different kinds of quasi-brittle materials are currently being performed to test our predictions.

-
- ¹ Z.P. Bažant, J. Eng. Mech. **110**, 518 (1984).
² Z.P. Bažant, Appl. Mech. Rev. **50** (10), 593 (1997) and references therein.
³ W. Weibull, Proc. Royal Swedish Inst. of Eng. Res. (Ingeniors Vetenskaps Akademien) **153**, 1 (1939)
⁴ M. Hori, and S. Nemat-Nasser, J. Mech. Phys. Solids **35** (5), 601 (1987).
⁵ M. Kachanov, Adv. in Appl. Mech. **30**, 259 (1994).
⁶ B.R. Lawn, *Fracture of Brittle Solids*, (2nd ed, Cambridge University Press, Cambridge, England, 1993)
⁷ A.B. Mosolov, Europhys. Lett. **24** (8), 673 (1993).
⁸ A. Carpinteri, Int. J. Solids Struct. **31** (3), 291 (1994).
⁹ E. Bouchaud, and J.-P. Bouchaud, Phys. Rev. B **50** (23), 17752 (1994).
¹⁰ A.S. Balankin, Int. J. Fract. **76**, R63 (1996).
¹¹ F.M. Borodich, J. Mech. Phys. Solids. **45** (2), 239 (1997).
¹² Z.P. Bažant, Int. J. Fract. **83**, 41 (1997).
¹³ S. Morel, J. Schmittbuhl, E. Bouchaud, and G. Valentin, Phys. Rev. Lett. **85** (8), 1678 (2000)
¹⁴ R.H. Dauskardt, F. Haubensak, and R.O. Ritchie, Acta Metall. Mater. **38** (2), 143 (1990).
¹⁵ E. Bouchaud, G. Lapasset, and J. Planés, Europhys. Lett. **13**, 73 (1990).
¹⁶ F. Plouraboué, P. Kurowski, J.-P. Hulin, S. Roux, and J. Schmittbuhl, Phys. Rev. E **51**, 1675 (1995).
¹⁷ J. Schmittbuhl, S. Roux, Y. Berthaud, Europhys. Lett. **28** (8), 585 (1994).
¹⁸ J.M. López, J.Schmittbuhl, Phys. Rev. E **57**, 6405 (1998).
¹⁹ T. Engøy, K.J. Måløy, A. Hansen, and S. Roux, Phys. Rev. Lett. **73** (6), 834 (1994).
²⁰ S. Morel, J. Schmittbuhl, J.M. López, and G. Valentin, Phys. Rev. E **58** (6), 6999 (1998).
²¹ E. Bouchaud, J. Phys. Cond. Mat. **9**, 4319 (1997).
²² S. Das Sarma, S.V. Ghaisas, and J.M. Kim, Phys. Rev. E **49** (1), 122 (1994).
²³ J.M. López, M.A. Rodríguez, R. Cuerno, Phys. Rev. E. **56** (4), 3993 (1997).
²⁴ F. Family and T. Vicsek, *Dynamics of fractal surfaces* (World Scientific, Singapore, 1991).
²⁵ Z.P. Bažant, Int. J. Fract. **83**, 19 (1997).
²⁶ Z.P. Bažant, M.T. Kazemi, J. Am. Ceram. Soc. **73** (7), 1841 (1990).
²⁷ C.M. Bender and S.A. Orszag, *Advanced Mathematical Methods for Scientists and Engineers*, chapters 9-11 (Springer-Verlag, New-York, 1999).

FIG. 1. Size effect on the critical resistance to crack growth G_{RC} obtained in the case of an anomalous scaling ($\zeta = 1.3$, $\zeta_{loc} = 0.8$, $A = 0.1$ and $l_o = 1$: arbitrary values)

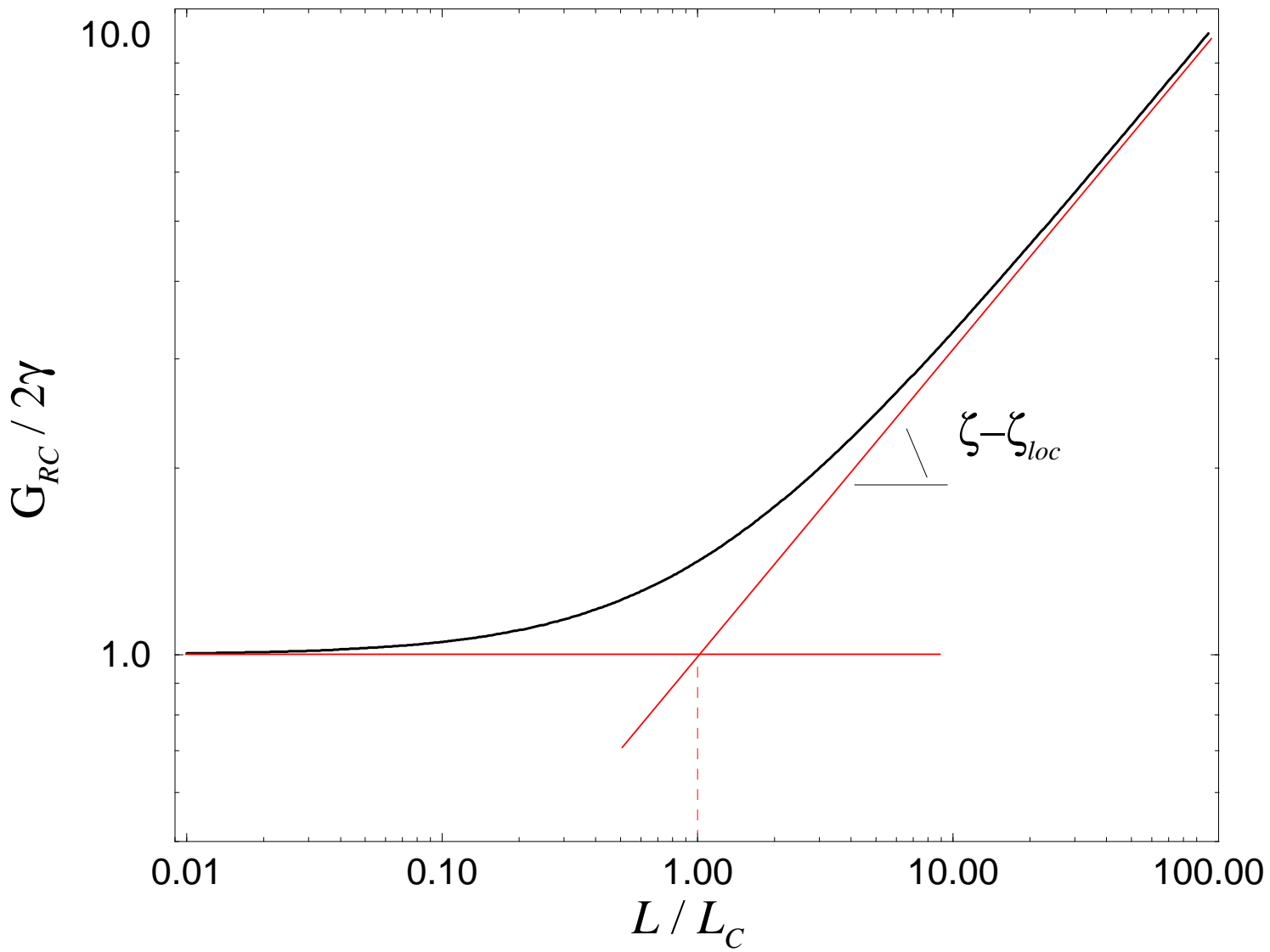
FIG. 2. Geometrically similar Tapered Double Cantilever Beam (TDCB) fracture specimens of different sizes $L = 7.5, 11.3, 15.0, 22.5, 30.0$ and 60.0 mm.

FIG. 3. Approximate size effect on the nominal strength (solid curve, Eq. (20)) and asymptotic series expansions (dashed curves, Eq. (13) and Eq. (18))

FIG. 4. Examples of R -curves $G_R(\Delta a)$ respectively obtained for pine (a) and spruce (b) from specimens of characteristic size $L = 11, 3$ mm.

FIG. 5. Size effect on critical energy release rate G_{RC} respectively for pine (a) and spruce (b). The expected slopes from the roughness analysis²⁰ are $\zeta - \zeta_{loc} = 0.47 \pm 0.17$ for pine (a) and 0.73 ± 0.17 for spruce (b).

FIG. 6. Size effect on nominal strength respectively for pine (a) and spruce (b). The expected slopes from the roughness analysis²⁰ are $-\frac{1}{2} + \frac{\zeta - \zeta_{loc}}{2} = -0.27 \pm 0.09$ for pine (a) and -0.14 ± 0.09 for spruce (b).



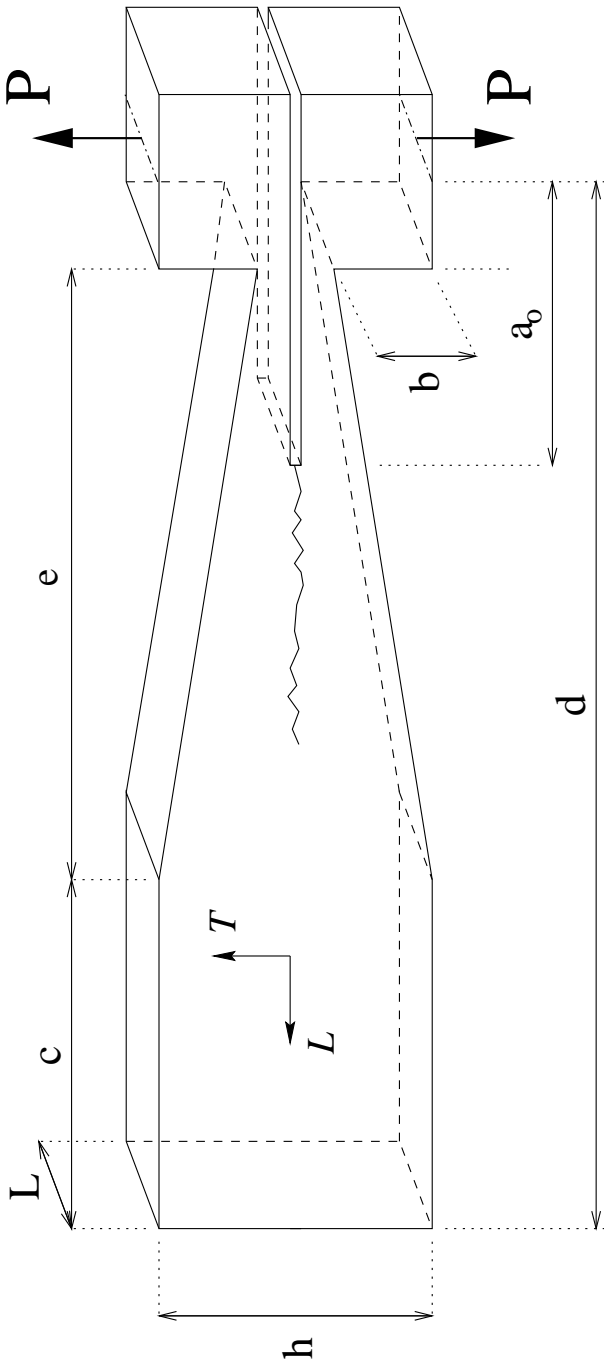


Figure2-Morel et al.-PRB

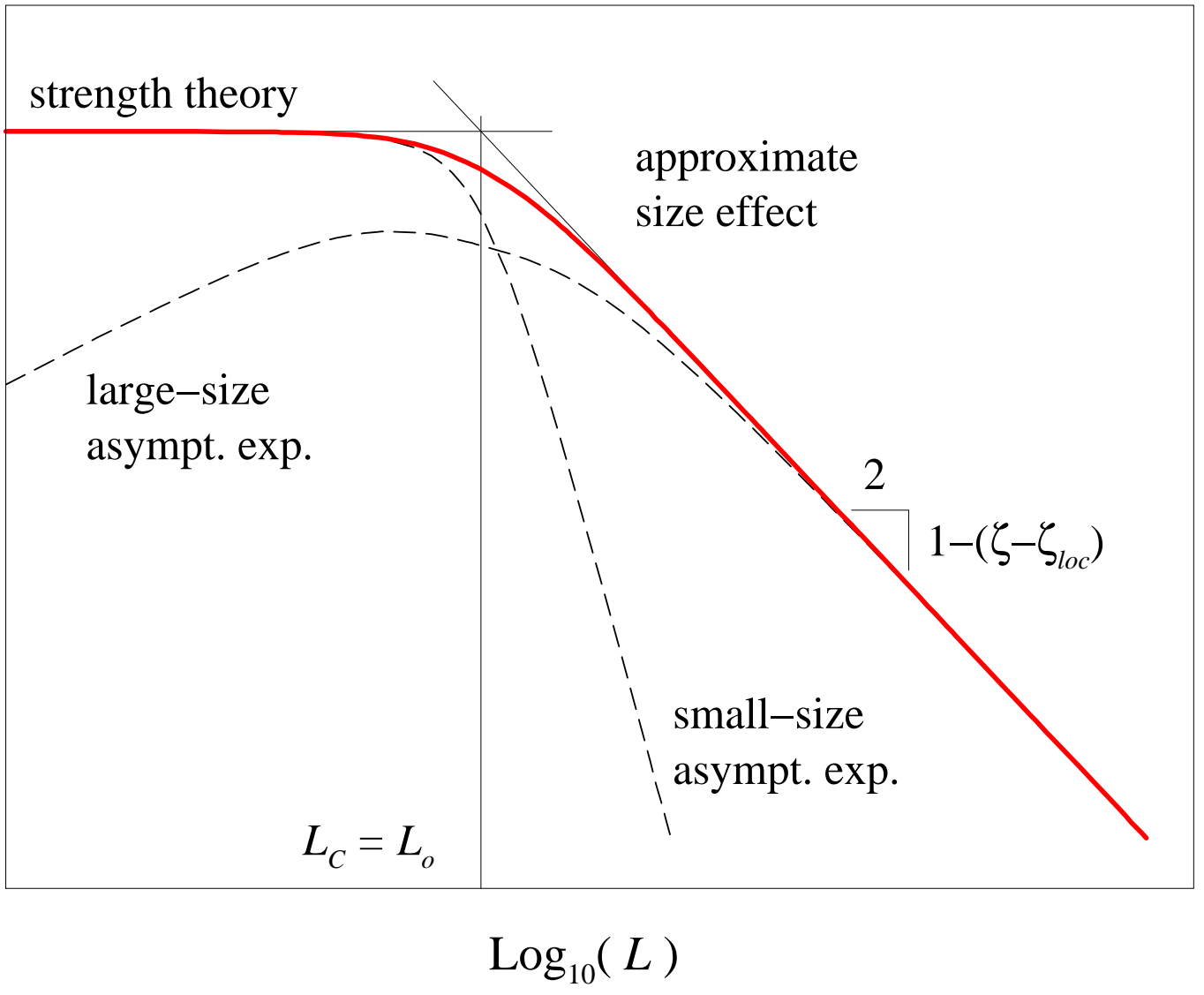


Figure3-Morel et al.-PRB

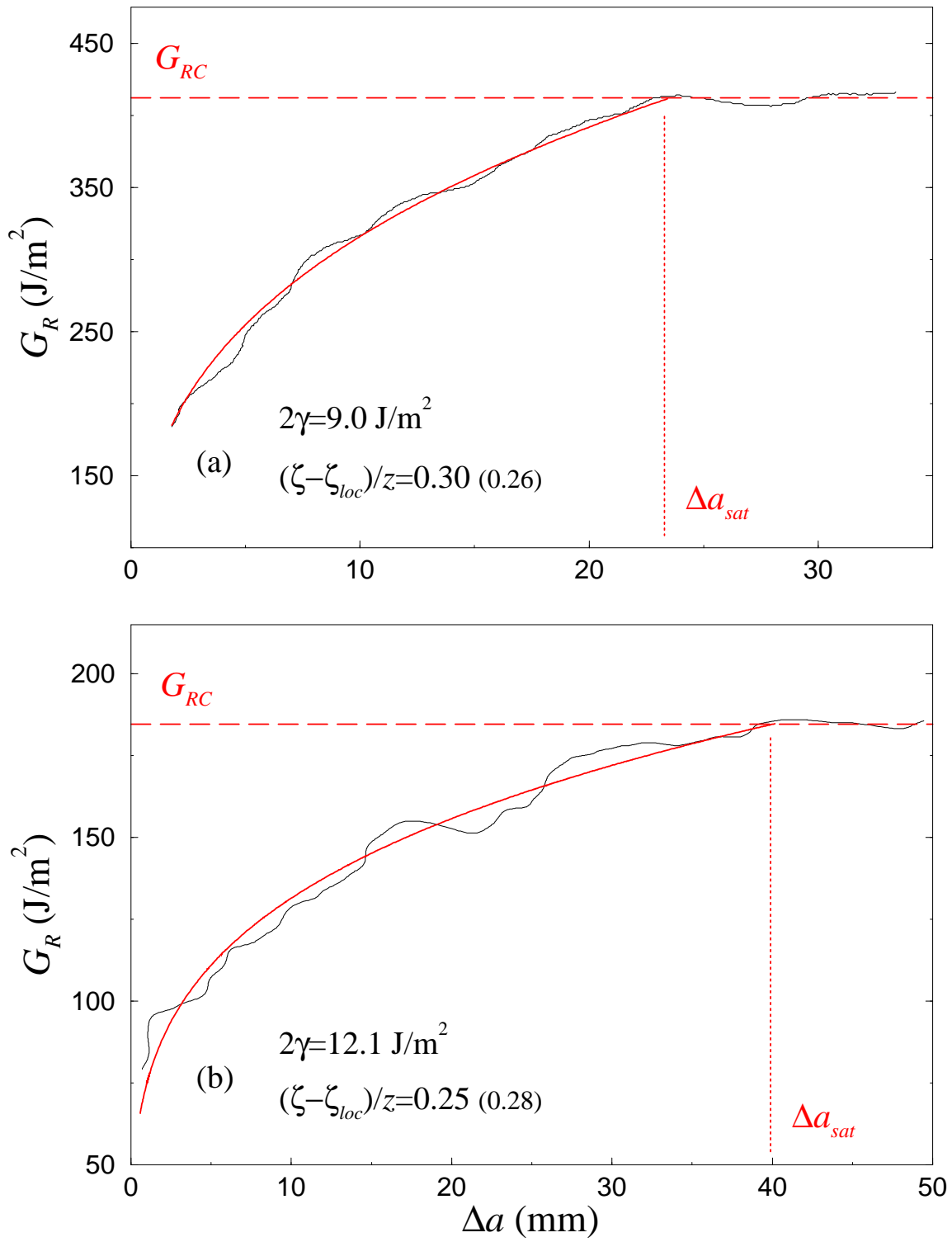


Figure4-Morel et al.-PRB

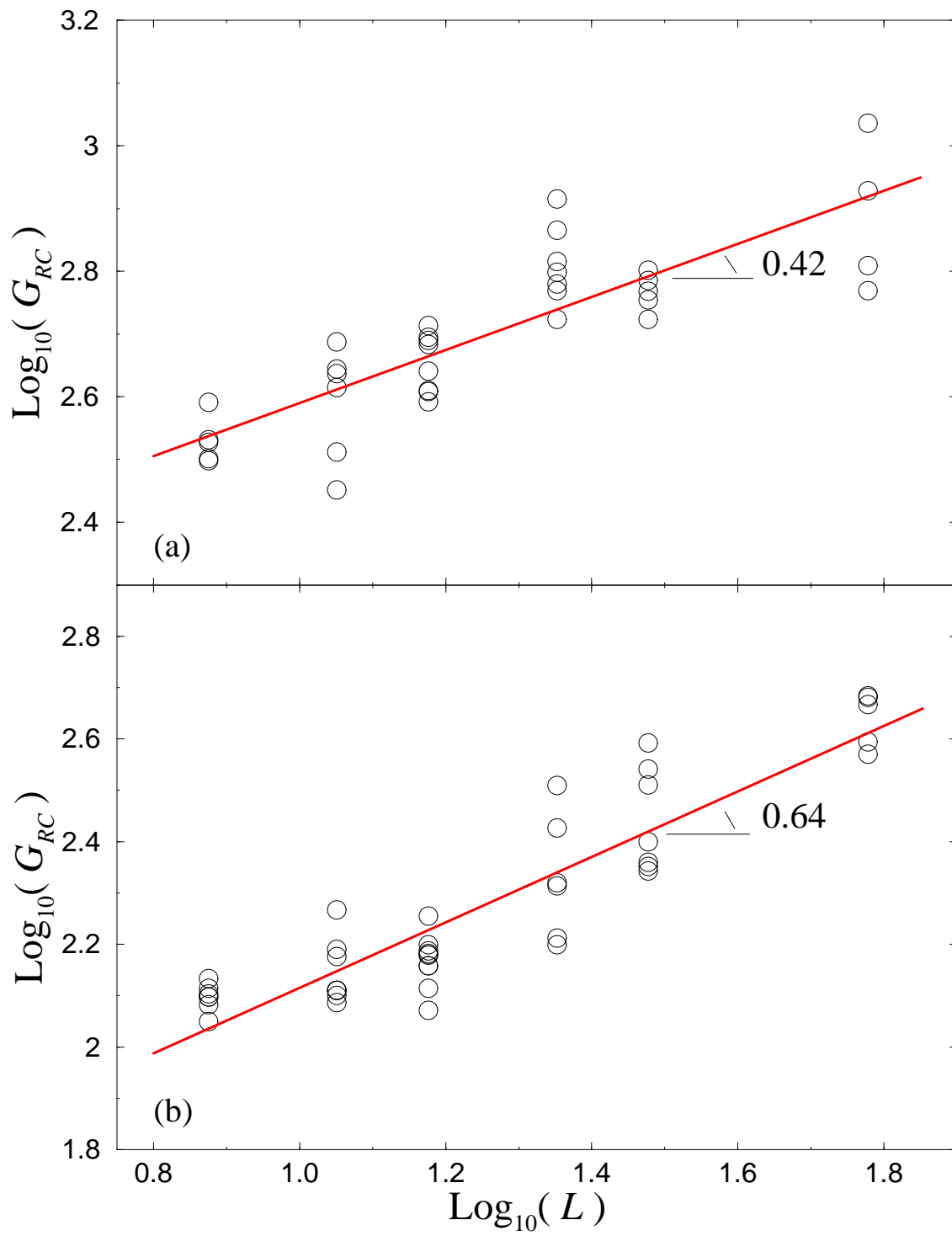


Figure5-Morel et al.-PRB

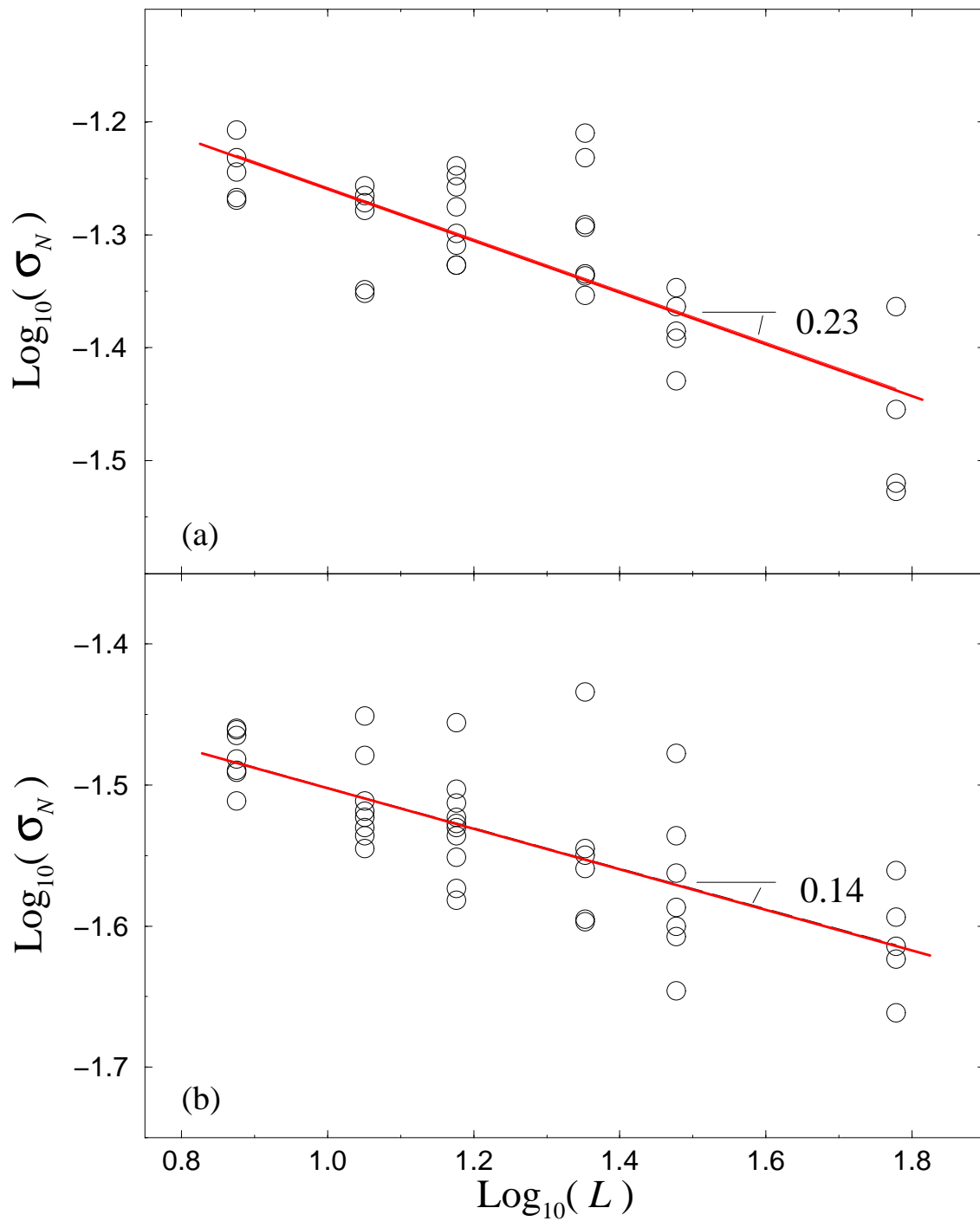


Figure6-Morel et al.-PRB